Cell Reports

Article

Energy Scarcity Promotes a Brain-wide Sleep State Modulated by Insulin Signaling in *C. elegans*

Graphical Abstract

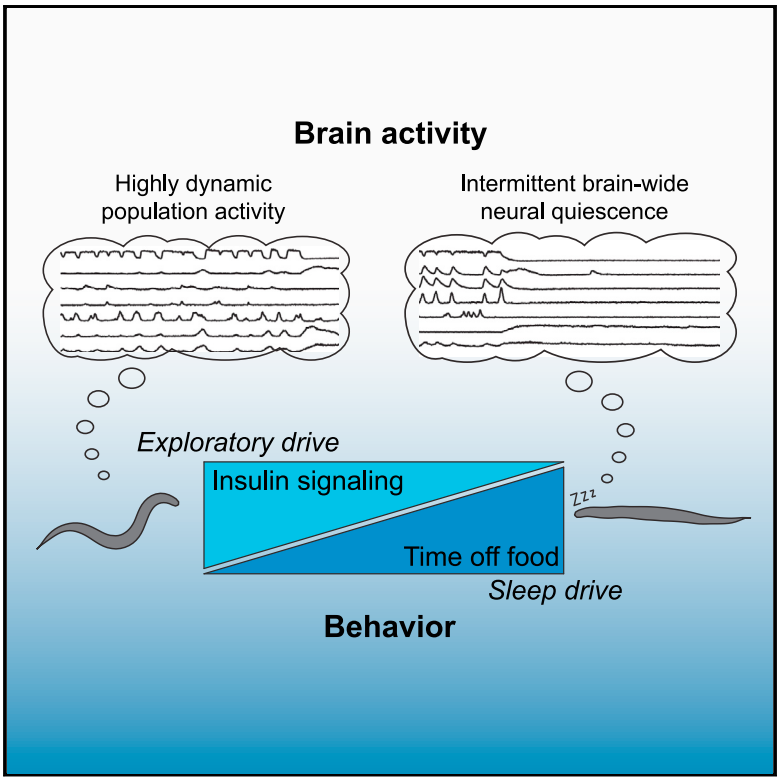

Authors

Susanne Skora, Fanny Mende, Manuel Zimmer

Correspondence

manuel.zimmer@imp.ac.at

In Brief

Skora et al. show in *C. elegans* that upon acute food deprivation, insulin signaling contributes to transient arousal, which declines with long-term starvation, hence permitting episodic sleep. During the remaining episodes of wakefulness, the brain maintains dynamic network activities. Sleep thus potentially serves an adaptive function in response to energy scarcity.

Highlights

- Starvation shifts the behavioral strategy from exploration to intermittent sleep
- Brain-wide neuronal population dynamics are robust to starvation
- Neuromodulation via insulin signaling maintains wakefulness during short fasting
- The insulin receptor DAF-2 acts in a network of sensory neurons and interneurons

Skora et al., 2018, Cell Reports *22*, 953–966
January 23, 2018
https://doi.org/10.1016/j.celrep.2017.12.091

CellPress

Cell Reports
Article

Energy Scarcity Promotes a Brain-wide Sleep State Modulated by Insulin Signaling in *C. elegans*

Susanne Skora,[1] Fanny Mende,[1,2] and Manuel Zimmer[1,3,*]
[1]Research Institute of Molecular Pathology (IMP), Vienna Biocenter (VBC), Campus-Vienna-Biocenter 1, 1030 Vienna, Austria
[2]Present address: Roche Pharmaceutical Research and Early Development, Roche Innovation Center Zurich, Roche Glycart AG, Wagistrasse 10, 8952 Schlieren, Switzerland
[3]Lead Contact
*Correspondence: manuel.zimmer@imp.ac.at
https://doi.org/10.1016/j.celrep.2017.12.091

SUMMARY

Neural information processing entails a high energetic cost, but its maintenance is crucial for animal survival. However, the brain's energy conservation strategies are incompletely understood. Employing functional brain-wide imaging and quantitative behavioral assays, we describe a neuronal strategy in *Caenorhabditis elegans* that balances energy availability and expenditure. Upon acute food deprivation, animals exhibit a transiently elevated state of arousal, indicated by foraging behaviors and increased responsiveness to food-related cues. In contrast, long-term starvation suppresses these behaviors and biases animals to intermittent sleep episodes. Brain-wide neuronal population dynamics, which are likely energetically costly but important for behavior, are robust to starvation while animals are awake. However, during starvation-induced sleep, brain dynamics are systemically downregulated. Neuromodulation via insulin-like signaling is required to transiently maintain the animals' arousal state upon acute food deprivation. Our data suggest that the regulation of sleep and wakefulness supports optimal energy allocation.

INTRODUCTION

The evolution of brains is constrained by the need for energy efficiency (Laughlin, 2001), yet brains remain among the most energy-consuming organs (Mink et al., 1981). This peculiarity of nervous systems might originate from a fundamental physical principle (Landauer's principle) that assigns a lower bound of energy consumption to computations (Landauer, 1961), rendering information-processing systems, such as brains, energetically costly. Therefore, brain operations must be contingent upon a tight balance between energy expenditure and conservation. Although there is an increasing body of knowledge delineating the brain circuitries that regulate appetite, food intake, and metabolism (Waterson and Horvath, 2015), much less is known about adaptive neuronal mechanisms that govern energy efficiency of neuronal processing.

Previous studies in insects suggest that neuronal processing is compromised when energy supply is scarce (Longden et al., 2014; Plaçais and Preat, 2013). Acute food deprivation in flies enhances arousal (Keene et al., 2010), but resistance to chronic starvation is associated with increased sleep (Slocumb et al., 2015). A similar yet less well-defined transition from initial arousal to elevated sleep levels is reported for rodents (Alvarenga et al., 2005), suggesting common adaptive mechanisms across animal phyla. However, the underlying systemic changes in neuronal activity patterns, and the neuromodulatory pathways that could regulate such neuronal adaptations are largely unknown. We propose here that studying behavior and brain activity under a strict regime of energy deprivation should directly reveal such adaptive mechanisms.

The nematode *C. elegans* is ideally suited for such studies. An array of behavioral paradigms has been established to measure behavioral adaptations to food deprivation; among these are chemotactic responses to ambient oxygen (O_2) levels (Zimmer et al., 2009). *C. elegans* inhabits rotten material in soil (Frézal and Félix, 2015), an environment where local fluctuations in O_2 potentially indicate the presence of bacterial food (Gray et al., 2004; Hums et al., 2016; Sexstone et al., 1985). Action commands are encoded in the worm brain by coordinated neuronal network dynamics, involving approximately 40% of all head neurons (Kato et al., 2015; Schrödel et al., 2013). These dynamics are systemically downregulated during developmentally timed sleep (termed lethargus) (Nichols et al., 2017). Taken together, these studies suggest that arousal and sleep in worms largely differ in their energy demands.

Here, we show that progressive energy deprivation of *C. elegans* is associated with an initial state of arousal followed by increasing pressure to enter reversible episodes of sleep. Unexpectedly, brain-wide network dynamics are robust to energy scarcity following starvation but become interspersed with short episodes of sleep. These data suggest that network dynamics are critical for neuronal function and that short bouts of sleep contribute to energy conservation, by reducing both brain and muscle activity. Starvation-induced sleep requires the FOXO transcription factor DAF-16. Its inhibition via the conserved insulin/IGF-1 pathway in a sensory neuron-interneuron network suppresses sleep during the initial arousal phase. We propose that neuromodulatory control of sleep and arousal via insulin signaling serves as an adaptive strategy to cope with energy deficits.

RESULTS

Arousal State Changes over the Time Course of Food Deprivation

We employed a previously reported population assay in which worms crawling freely on agarose perceive rapid temporal shifts in O_2 concentration from atmospheric 21% to intermediate 10% O_2 (henceforth "O_2 downshift") (Zimmer et al., 2009). Using this paradigm, we previously reported that 1-hr food-deprived worms (henceforth "fasted") elicit a sustained switch in behavioral strategy from long-distance travel (LDT) prevalent at 21% O_2 to sustained area-restricted search (ARS)-like behavior at 10% O_2 (Hums et al., 2016). A food deprivation time course that extends from 15 min off food ("well-fed") to severe starvation (16 hr off food, "starved") revealed a gradual change in behavioral strategy (Figures 1A–1D and S1A): whereas well-fed animals only briefly reduced locomotion speed in response to O_2 downshift (Figures 1A and 1B), fasted animals exhibited the prolonged slowing and backward-crawling (reversal) response previously extensively characterized as ARS behavior (Figures 1A and 1B) (Hums et al., 2016). This difference in fasted versus well-fed behavior demonstrates an enhanced behavioral responsiveness of fasted animals toward intermediate O_2 concentrations. As a condition of severe starvation, we chose 16 hr off food. At this point, animals have already largely reduced their fat resources (Witham et al., 2016) and retained eggs. However, larvae did not yet hatch internally, which could impact the mother animals. Upon starvation, the O_2 downshift-evoked reversal response was attenuated and slowing was sustained, i.e., no speed recovery was observed throughout the 6-min period at low O_2 (Figures 1A and 1B). In addition, starved animals responded to O_2 downshift with transient episodes of motor inactivity that either affected the whole body (henceforth "quiescence") (Figure 1C), or were characterized by retained movement of the head-neck region (henceforth "head-waving") (Figures 1D and S1B; Movie S1). While quiescence was defined as a discrete behavioral state by the absence of any motion above the detection threshold of our method, we observed a smooth change in movement parameters from active forward crawling to head-waving (Figure S1C). Such a gradual adjustment of movement parameters was described previously (Gallagher et al., 2013; Hums et al., 2016). However, in order to quantify in parallel all observed behavioral features, in the present study we simplify and treat head-waving as a discrete category. Here, head-waving is defined by the absence of detectable crawling while movement remains apparent in anterior body parts (Figure S1B; Movie S1; see also Experimental Procedures). Quiescence and head-waving were immediately and completely suppressed by a subsequent O_2 upshift to 21%. Well-fed and fasted animals lacked quiescence and head-waving (Figures 1C and 1D).

In summary, during a food deprivation time course animals initially increased arousal levels, evidenced by elevated behavioral responsiveness, which was followed by a progressive propensity to enter reversible episodes of quiescence.

A Sensory Circuit Involved in O_2 Modulation of Starvation Quiescence

We next used genetic cell ablation strains to probe the neural requirements for quiescence and head-waving behavior in response to O_2 shifts. O_2 downshift activates O_2-sensory neurons of the BAG class (Zimmer et al., 2009), whereas O_2 upshift activates sensory neurons of the URX, AQR, and PQR classes (Persson et al., 2009; Zimmer et al., 2009). Surprisingly, quiescence was independent of BAG neurons but depended strongly on URX, AQR, and PQR neurons. Ablating all of these classes of O_2-sensing neurons did not suppress quiescence further (Figure S1D). RMG interneurons are central to a gap junction circuit of nociceptive, pheromone, and URX O_2 sensory neurons (Macosko et al., 2009) (Figure S1F). This circuit was shown to relay arousal signals from nociceptive (Choi et al., 2015) and O_2-sensory neurons (Nichols et al., 2017). Animals lacking RMG neurons showed reduced quiescence (Figure S1D) and head-waving (Figure S1E). Notably, the RMG cell ablation was the only one that affected O_2 downshift modulation of head-waving behavior (Figure S1E). Almost complete suppression of both quiescence and head-waving could be achieved by broadly disrupting sensory neuron-dependent signaling using animals mutant in the transient receptor potential channel V (TRPV) OSM-9 (Colbert et al., 1997) (Figures S1D and S1E). This indicates that sensory signals, likely from several neurons, are necessary for quiescence and head-waving episodes. The effect of RMG ablation on head-waving might thus be explained by either its role as a hub neuron downstream of several *osm-9*-expressing sensory neurons (Figure S1F) or via its potential role as motor neuron innervating muscles in the head (White et al., 1986). Surprisingly, none of the known O_2 upshift-sensing neurons and molecular O_2 upshift sensors was required for the acute arousal response upon O_2 upshift (Figure S1G).

In summary, starvation quiescence is under control of a sensory neuron-interneuron network including the hub interneuron RMG.

Acute Changes in Ambient O_2 Levels Transiently Modulate Behavioral State Transitions

In accordance with previous studies (Ghosh and Emmons, 2008; McCloskey et al., 2017), we found that starvation-induced quiescence also occurred independent of acute O_2 switches when animals were left unperturbed in the absence of food for at least 10 hr at constant 21% O_2 (Figure S2A). Furthermore, in longer-term (130-min) experiments on prior starved animals, quiescence was initially suppressed but reached steady-state levels after ~30 min (Figures 1E and 1F). This indicated that intermediate O_2 concentrations as used in our initial experiments (Figures 1A–1D) were likely to serve a modulatory function for a default starvation-dependent behavior rather than being permissive. It furthermore suggested that the handling prior to experiment start (i.e., moving of assay plates and initiation of O_2 flow) caused transient arousal of the worms. Once steady-state levels of quiescence had been established, acute O_2 downshifts or upshifts transiently modulated quiescence and head-waving behavior (Figures 1E and 1F).

We next used the identification of active, quiescent, and head-waving episodes to investigate the sequences of behavioral transitions and their modulation by O_2 shifts. Using the experiments shown in Figures 1E and 1F, we calculated state transition rates during steady-state periods at both 21% and 10% O_2, and upon O_2 shifts. The only significant difference between steady states

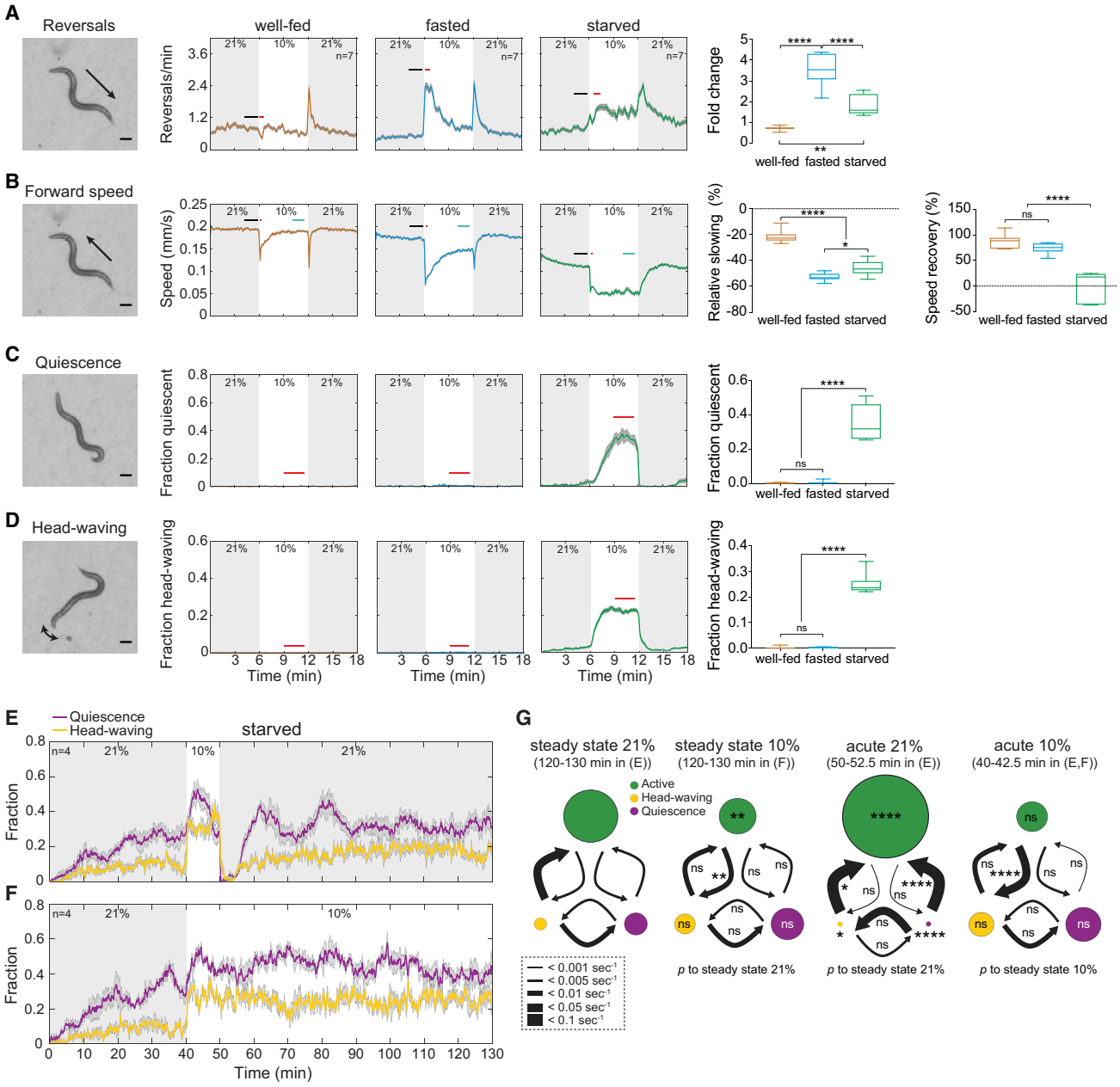

Figure 1. Change in Arousal State over the Time Course of Food Deprivation

(A–D) Pictures on the left show single video frames of WT worms during indicated behavior. Scale bars: 100 μm. Traces show population means (±SEM) across experiments under indicated feeding states for reversals (A), forward speed (B), quiescence (C), and head-waving behaviors (D). Animals were stimulated with changing O_2 concentrations as shown. n indicates number of experiments (~100 animals each). Bars denote time intervals used for quantifications on the right. Boxplots (median, interquartile range, and min to max whiskers) on the right show quantifications of fold- or %-change (red- versus black-labeled intervals) in reversal frequency and speed. Speed recovery is the %-change during cyan- versus red-labeled intervals relative to basal levels (black bar). Mean fraction quiescent or head-waving during red-labeled intervals. One-way ANOVA with Tukey's correction was used to compare all conditions against each other (****$p < 0.0001$, ***$p = 0.0009$, **$p = 0.0019$; ns, $p > 0.05$).

(E and F) Population means (±SEM) of fraction starved WT worms in quiescent (purple) or head-waving (yellow) state during longer recordings. O_2 concentration as indicated. n indicates number of experiments (~50 animals each). (F) Same as (E) but using different O_2 stimulation, as indicated.

(G) State transition rates calculated from (E) and (F). Arrow thickness show mean outbound transition rates according to legend in dashed box. Diameter of circles: mean state probability. Conditions were compared as indicated below panels using multiple t tests with Holm-Sidak correction (****$p < 0.0001$, **$p \leq 0.01$, *$p \leq 0.05$; ns, $p > 0.05$).

See also Figures S1 and S2 and Movie S1.

at chronic 10% versus 21% O_2 was an increase in the transition rate from active locomotion to head-waving (Figure 1G). Acute O_2 downshift further increased the transition rate from activity to head-waving while leaving other state transition rates unchanged. Thus, O_2 downshift promoted quiescence solely by elevating the prevalence of the head-waving state, which could thus be interpreted as a permissive prior state for quiescence (Figure 1G) that leads to a typical behavioral sequence of active → head-waving → quiescence. O_2 upshift affected all measured transitions, causing active locomotion to transiently prevail (Figure 1G). In conclusion, acute changes in ambient O_2 levels transiently modulated the extent of quiescence with respect to pre-stimulus levels, but none of the concentration ranges tested in this study was either strictly permissive or prohibitive for quiescence.

Starvation Quiescence Is a Behavioral Sleep State

Previously reported quiescent states in *C. elegans* fulfil criteria for sleep: reversibility, locomotion and feeding quiescence, specific posture, increased arousal thresholds, and homeostasis (Hill et al., 2014; Iwanir et al., 2013; Raizen et al., 2008). An assessment of whether starvation quiescence qualifies as sleep state, however, has been lacking. Reversibility occurred either via spontaneous switching (Figure 1G) or following O_2 upshift (Figure 1C). We next inspected feeding, i.e., pharyngeal pumping activity, in individual starved animals under a stereomicroscope and observed that, unlike during active or head-waving episodes, quiescence was devoid of feeding (Figure S2B).

We measured body postures via a shape factor (eccentricity) and found that quiescent worms were more straightened than worms during forward movement (Figure S2C).

Upon O_2 upshift, active worms responded with a strong acute reversal response whereas quiescent worms solely resumed to baseline reversal rates (Figure S2D), indicating reduced sensory responsiveness.

We found a small but highly significant correlation between the lengths of quiescence bouts and preceding active bouts (Figure S2E), indicating a minor homeostatic component to the quiescence drive. Notably, no significant correlation was found between other combinations of successive behavioral states (Figures S2F–S2H).

In conclusion, starvation quiescence fulfils the behavioral criteria to classify as sleep.

The Insulin Receptor DAF-2 Acts in a Sensory Neuron-Interneuron Network to Maintain an Arousal State upon Fasting

We conducted a candidate genetic screen in fasted animals and identified mutant strains showing quiescence prematurely upon fasting (Table S1). The most intriguing gene was *daf-2*, which encodes for the sole *C. elegans* homolog of the insulin/IGF-1 receptor (Kimura et al., 1997). Insulin signaling is known to affect quiescent states in both developing and adult animals (Gems et al., 1998) and has recently been suggested to modulate quiescence behavior in starved animals (McCloskey et al., 2017). Under our conditions, the *daf-2* mutation specifically affected the timescale of behavioral adaptation to food deprivation: *daf-2* fasted animals behaved like wild-type (WT) starved animals (Figures 2A and S3A). *Daf-2* animals have been reported to have reduced food ingestion rates (e.g., Dillon et al., 2016; Dwyer and Aamodt, 2013; McCloskey et al., 2017), a defect that could result in a chronic starvation state and lead to the display of a starved behavioral phenotype. However, quiescence of *daf-2* animals required the 1-hr off-food fasting period as it was not observed when well-fed (Figure 2A). Furthermore, our candidate genetic screen included animals with severe reductions in food intake (*eat-2* [Raizen et al., 1995], *tph-1* [Sze et al., 2000]), which did not display quiescence (Table S1). Nevertheless, we assayed feeding rates in *daf-2* animals under our cultivation conditions and found that *daf-2* mutants displayed only a mild reduction in pharyngeal pumping frequency (Figure S3B). These findings suggest that reduced food ingestion is insufficient to cause the phenotype observed in *daf-2* fasted animals and that *daf-2* plays rather a direct role in the regulation of quiescence behavior. One major output of the *daf-2* signaling pathway is the FOXO transcription factor *daf-16*. Consistent with DAF-2 signaling inhibiting FOXO (Kimura et al., 1997), quiescence levels in fasted *daf-16; daf-2* double mutants corresponded to *daf-16* levels (Figures 2B and S3C). Moreover, both *daf-16* single and *daf-16;daf-2* double mutants exhibited low levels of quiescence upon starvation (Figure 2B), indicating that high *daf-16* signaling, i.e., low levels of *daf-2* signaling, are required for elevated sleep upon starvation. This genetic evidence strongly supports our interpretation that insulin signaling maintains a transient aroused state upon fasting and that a progressive decline in insulin signaling leads to elevated sleep levels upon starvation.

Daf-2 is widely expressed across tissues (Cao et al., 2017); however, as assessed by transgenic rescue experiments using tissue-specific promoter fragments, maintenance of ARS behavior, indicated by sustained reversal and slowing responses, as well as arousal upon fasting could be restored by *daf-2* expression solely in the nervous system (using *Prab-3*) (Figures 2C and S3D). More specifically, arousal upon fasting could be partially restored by expressing *daf-2* either broadly in interneurons and motor neurons (using *Pglr-4*) or broadly in sensory neurons (using *Posm-9*, Figure 2C). The expression patterns of the *Pglr-4* and *Posm-9* promoters were assessed by confocal microscopy, yielding no overlap, and thus indicating that *daf-2* acts in a network that involves both sensory and interneurons. The top candidate neuron expressed under *Pglr-4* is the hub interneuron RMG. Expressing *daf-2* in RMG and a few other cells (using *Pflp-21*) restored quiescence levels similarly to *Pglr-4*. Expressing *daf-2* under both *Pflp-21* and *Posm-9* restored quiescence to levels comparable to WT (Figure 2C). Since *Pflp-21* and *Posm-9* overlapped in their expression in ASJ, ASJ is likely not critical for the observed additive effect. Exclusive expression of *daf-2* in URX, AQR, PQR, and ASI failed to affect quiescence (Figure S3E). We were unable to exclude significance of expression in URA or FLP, the only neurons besides RMG that were expressed under both *Pflp-21* and *Pglr-4*; however, the requirement of RMG for starvation-induced quiescence behavior (Figure S1D) and in the mediation of other arousal signals (Choi et al., 2015; Nichols et al., 2017) makes it a more likely candidate as a major site of *daf-2* action.

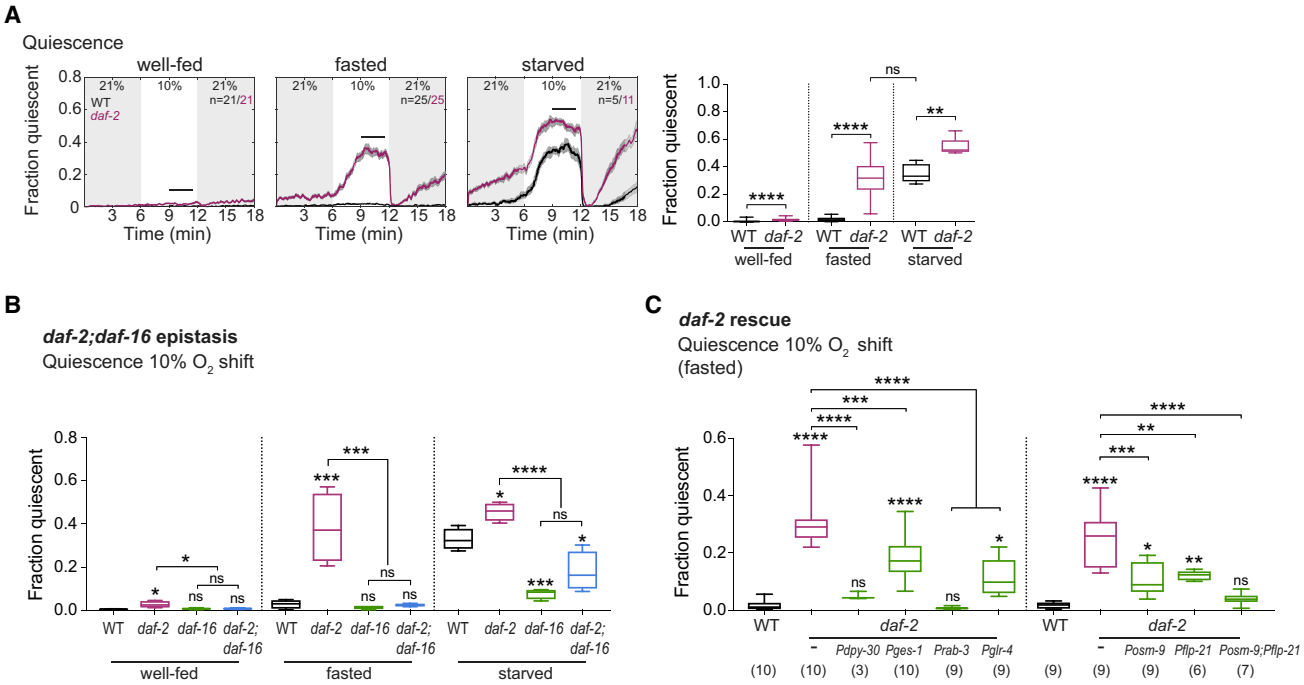

Figure 2. The Insulin Receptor DAF-2 Acts in a Sensory Neuron-Interneuron Network to Maintain Arousal upon Fasting

(A) Left: population means (±SEM) of quiescence behavior with O_2 stimulation under indicated feeding states. n indicates number of experiments (40–120 animals each). Right: quantifications using Mann-Whitney test (well-fed) or unpaired t test (others) (****$p < 0.0001$, **$p = 0.0018$; ns, $p = 0.7314$). n-numbers as indicated on the left, except *daf-2* starved, where only experiments performed in parallel to WT were used for quantification (i.e., n = 5).

(B) Quantification of *daf-2;daf-16* epistasis experiment for O_2 downshift-dependent quiescence under indicated feeding states, using one-way ANOVA with Tukey's correction (****$p < 0.0001$, ***$p < 0.001$, *$p \leq 0.05$; ns, $p > 0.05$). Significance against WT indicated above each boxplot. Additional comparisons as shown. Quantification interval as in Figure 2A. Number of experiments (n) = 4 each.

(C) Quantification of tissue- and cell-specific *daf-2* rescue experiments. *Pdpy-30*, ubiquitous; *Pges-1*, intestine; *Prab-3*, pan-neuronal; *Pglr-4*, interneurons and motor neurons; *Posm-9*, sensory neurons; *Pflp-21*, RMG, FLP, ASJ, M2, URA, URX, and ASI. Significance against WT indicated above each boxplot. Additional comparisons as shown. One-way ANOVA with Sidak's correction ****$p < 0.0001$, ***$p \leq 0.001$, **$p \leq 0.01$, *$p \leq 0.05$; ns, $p > 0.05$. Number of experiments (~40 animals each) below each boxplot.

WT and *daf-2* in (B) and (C) (left side) were controls performed in parallel but are subsets of the data in (A). WT and *daf-2* in (C) (right side) constitute a separate dataset. Boxplots show median, interquartile range, and min to max whiskers. See also Figure S3 and Table S1.

In summary, we identified the requirement for insulin signaling in both sensory neurons and interneurons in maintaining transient arousal upon fasting.

Starvation Promotes Periods of Global Neural Inactivity

We next sought to characterize the changes in brain activity that underlie the longer-timescale changes in behavior mediated by feeding state. We used a recently developed approach for brain-wide single-cell-resolution real-time Ca^{2+} imaging (Kato et al., 2015; Schrödel et al., 2013). Animals were immobilized in a microfluidic device allowing for high-resolution fluorescence microscopy and precise control of the gaseous environment (Zimmer et al., 2009). We previously reported that the brain activity of well-fed WT worms is dominated by global neuronal population dynamics, which arise from the coordinated activity involving a large fraction of all interneurons and motor neurons in the brain. Our previous work showed that these dynamics coordinate the generation of motor commands independent of movement, e.g., while animals are immobilized on the microscope stage (Kato et al., 2015). Here, we focused our efforts on the fasted and starved time points in order to characterize the changes in brain activity that underlie the frequent alternations between sleep and wakefulness. The imaging experiments employed the same protocol as used for behavioral experiments to switch between 21% and 10% O_2. We observed that starved, as opposed to fasted, worms frequently displayed periods of widespread downregulation of neuronal activity (Figures 3A–3C, S4A, and S4B). We used the brain state classifier validated during our previous work on lethargus sleep to quantify the occurrence of the episodes of neuronal downregulation: simultaneous inactivity of the AVA interneurons and the VB, SMD, and RIV motor neurons is a sufficient indicator of brain state episodes devoid of motor commands (Nichols et al., 2017). Applying this classifier to multiple recordings revealed that starvation was associated with an increased frequency of reversible quiescent brain state episodes (Figure 3D). While our imaging experiments recapitulated the frequent occurrence of quiescence upon starvation, we were unable to observe additional modulation by O_2 stimuli (compare Figures 3D and 3E). Similarly, we found that the O_2 stimulus did not elicit additional reversal commands (Figure S5). This is in contrast to our previous studies in well-fed animals, where we observed efficient stimulus-evoked motor

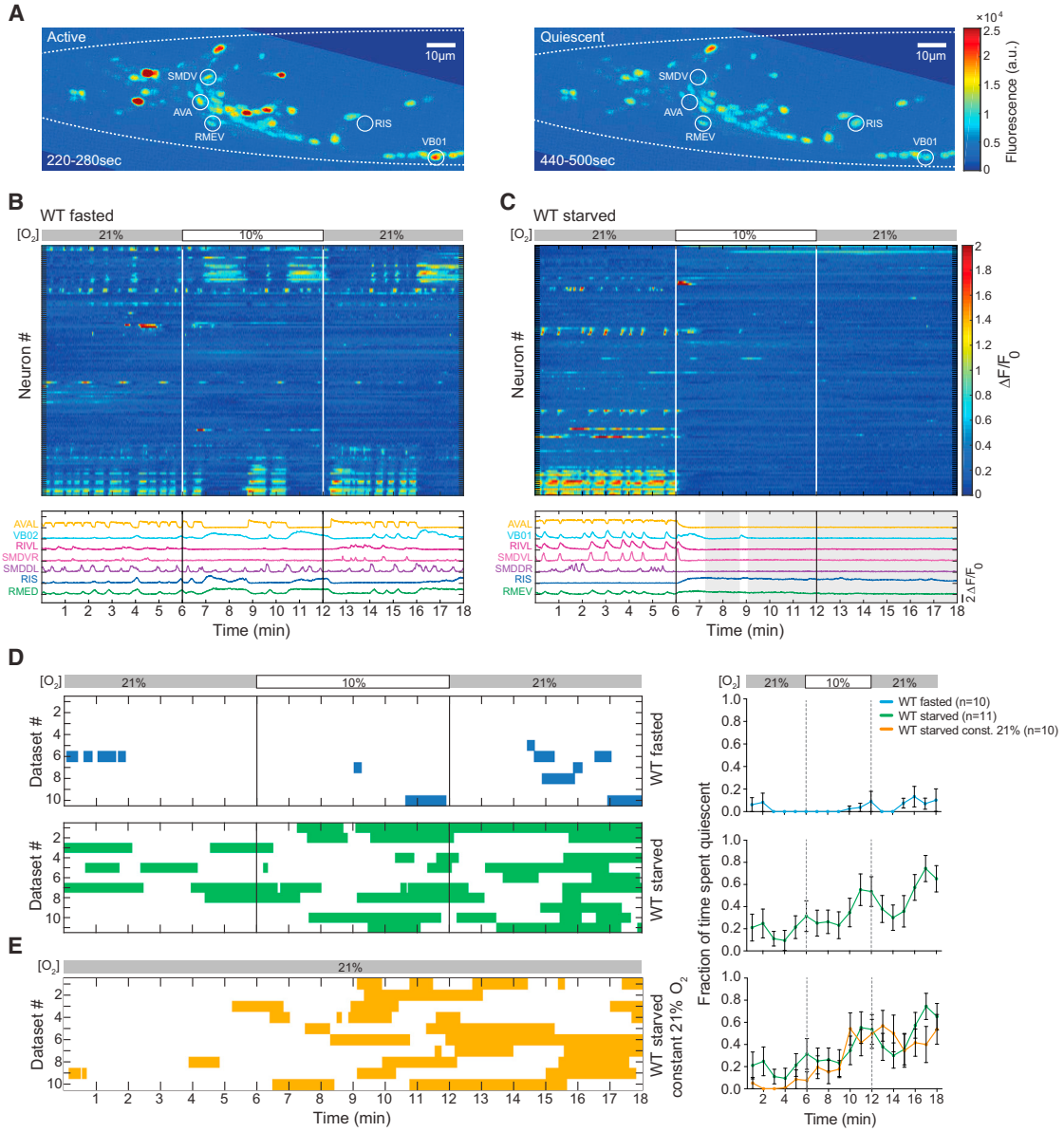

Figure 3. Starvation Promotes Episodes of Global Neural Inactivity

(A) Maximum intensity projections across the indicated time periods of the brain-wide imaging recording shown in (C). Selected neuronal classes are labeled.

(B and C) Heat plots of representative brain-wide imaging recordings for WT fasted (B) and WT starved (C) worms. O_2 stimulation as indicated. Rows are NLS-GCaMP5K fluorescence time series ($\Delta F/F_0$) of segmented head neurons, sorted by correlations. Example traces are shown below: reversal interneuron AVA, forward motor neurons VB02 or VB01, turning head motor neurons RIV, SMDV, and SMDD, and GABAergic neurons RIS and RMED/V. Grey shadings indicate quiescence periods.

(D and E) Left: brain state ethograms showing quiescence episodes of worms in brain-wide imaging recordings with O_2 stimulation as indicated. One row corresponds to one recording, each a different animal. Right: traces show mean (±SEM) fraction of time spent quiescent in 1-min bins, across all corresponding datasets shown on the left. n indicates number of recordings. (E) Same as (D) but at constant 21% O_2. Green traces in (D) and (E) on the right are the same data.

See Figures S4 and S5.

commands (Kato et al., 2015; Nichols et al., 2017). It is possible that fasted and starved worms are more affected by the confinement conditions in the device, leading to inefficient sensory-motor processing. Quiescence levels observed under these imaging conditions, however, followed a time course observed under basal freely behaving conditions (compare Figures 3D and 3E to first 20 min in Figures 1E and 1F). Therefore, our imaging results are most informative in the context of basal starvation quiescence but less so for O_2 modulation of quiescence behavior.

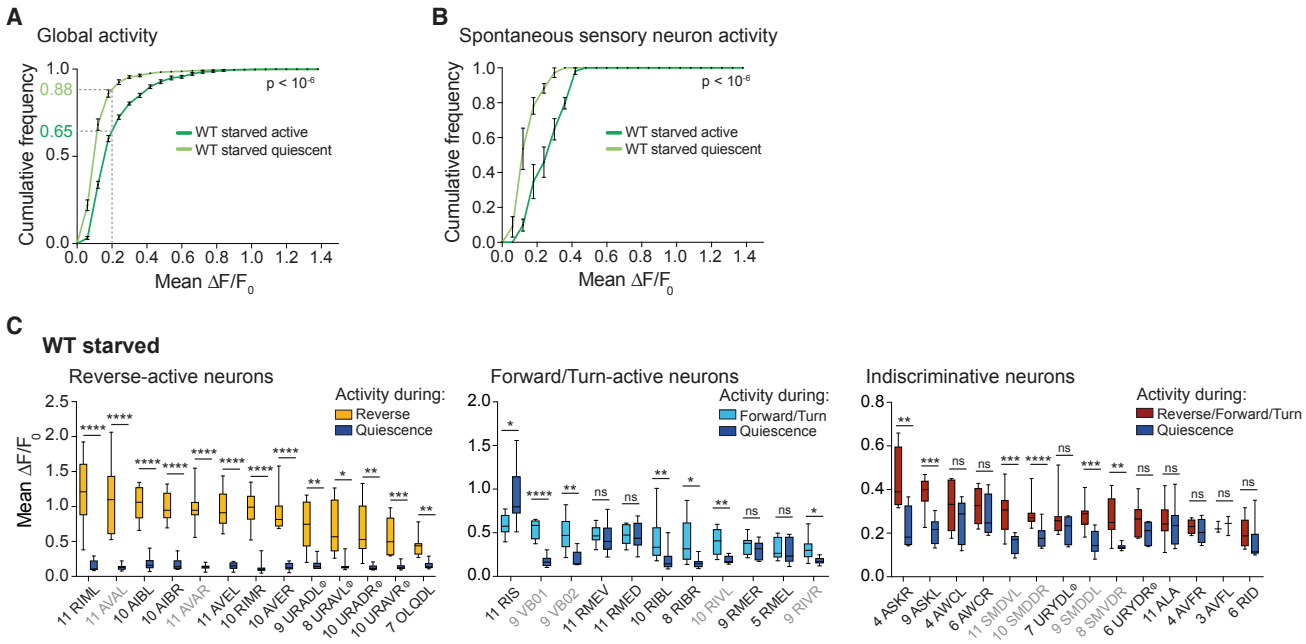

Figure 4. Sleep upon Starvation Recapitulates a Global Sleep Brain State

(A) Mean (±SEM) cumulative fractional distributions of mean $\Delta F/F_0$ values across all neurons (excluding O_2-responsive neurons) during active or quiescent episodes, in WT starved animals. Dashed gray lines denote a cutoff, below which neurons were usually found inactive. Number of recordings (n) = 6.

(B) Mean (±SEM) cumulative fractional distributions of mean $\Delta F/F_0$ values across spontaneously active sensory neurons during active or quiescent episodes. Number of recordings (n) = 6. The p values in (A) and (B) indicate the probability of obtaining an equal or higher difference between the distributions after random shuffling of quiescence episodes; see Experimental Procedures.

(C) Mean $\Delta F/F_0$ values of identified neurons during each neuron's principal active brain state (reverse, forward/turn, or active irrespective of motor state) and the quiescent brain state. Boxplots show median, interquartile range, and min to max whiskers. Labels indicate putative neuron IDs. Ambiguous IDs are labeled with Φ (see Experimental Procedures for alternatives). Number of data points for each neuron (n) indicated. Grayed neuronal classes were used for classification of quiescent brain states. Paired t tests (****$p < 0.0001$, ***$p \leq 0.001$, **$p \leq 0.01$, *$p \leq 0.05$; ns, $p > 0.05$).

See also Figure S6.

Starvation Quiescence Features a Global Sleep Brain State

We continued to investigate the quiescent brain state in depth, to compare it to the recently described sleep brain state during lethargus. As a global measure of neuronal activity changes from active to quiescent brain episodes, we compared the cumulative distributions of mean $\Delta F/F_0$ values for all neurons, except O_2-responsive neurons, in WT starved worms. This analysis quantitatively confirmed our initial observation (see Figures 3A–3C and S4B) that quiescence resulted in a downregulation of neuronal activity on a global scale (Figure 4A). Specifically, during active brain states, around ~35% of neurons were engaged in neuronal activity while this number was decreased to ~10% during quiescence. This downregulation thus affected approximately three-quarters of all typically active neurons. Since neuronal population dynamics in *C. elegans* encode motor commands, the suppression of these activities is expected during a brain state that corresponds to locomotor quiescence. However, we discovered spontaneous motor-unrelated activity in a cluster of neurons in the anterior lateral ganglia. These comprise the cell types ASK, AFD, ADF, AWA, AWB, AWC, and ASH, all of which are sensory neurons. Except for ASK and AWC (see below), the exact cell types of these neurons were ambiguous in individual recordings. Therefore, we performed a global activity analysis as above but restricted to the spontaneously active neurons in this location: these spontaneous sensory neuron activities were also downregulated during quiescence (Figure 4B), showing that the quiescent brain state affects both the motor and sensory domains.

Next, we focused our analysis on the identifiable neuronal classes: most neuronal types that participated in population dynamics were downregulated during quiescence (Figure 4C). Remarkably, exceptions were GABAergic neuronal classes, notably the known sleep-promoting GABAergic and peptidergic neuron RIS (Turek et al., 2013, 2016), as well as the GABAergic head motor neuron class RME (composed of RMEL, RMER, RMEV, and RMED); these neurons retained stable Ca^{2+}-plateaus during quiescence. Moreover, the GABA uptake neuron AVF (Gendrel et al., 2016) and the GABA-and peptidergic interneuron class ALA (Gendrel et al., 2016) also remained active (Figures 4C and S4B). Spontaneously active sensory neurons were differentially affected, with some sensory neuron types downregulated during quiescence (ASK, Figure 4C) while others retained their activity (AWC, Figure 4C). Therefore, brain activity during starvation quiescence does not simply reflect absence of behavior-related activity but exhibits a specific neuronal signature.

Our recent work showed that neuronal population dynamics in *C. elegans* can be visualized using principal component analysis

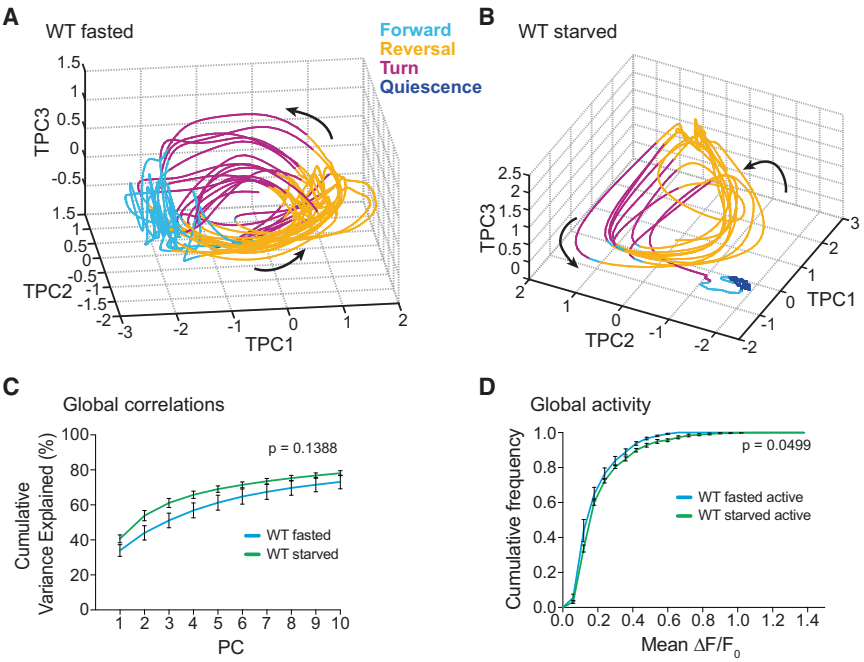

Figure 5. Neural Population Dynamics Are Robust to Starvation

(A and B) Phase plots of first three temporal principal components (TPCs) for the WT fasted (A) and WT starved (B) datasets shown in Figures 3B and 3C. Coloring indicates the respective motor command state, and arrows indicate the direction of time. More examples are shown in Figures S4A and S4B.

(C) Mean (±SEM) cumulative variance explained by first ten PCs during active brain state episodes.

(D) Mean (±SEM) cumulative fractional distributions of mean $\Delta F/F_0$ values across all detected neurons (excluding O_2-responsive neurons) during active brain state episodes. The p values in (C) and (D) indicate the probability of obtaining an equal or higher difference between the distributions after random shuffling; see Experimental Procedures. Number of recordings (n) = 6 each.

See also Figure S4 and Movie S2.

(PCA) as a dimensionality reduction method. PCA phase plots highlight the recurrent feature of brain dynamics, i.e., the brain state evolves through a stereotypic and repeating pattern of fluctuating but highly coordinated network activity. These dynamics correspond to a motor command sequence: forward crawling–reversal–dorsal or ventral turn (Kato et al., 2015) (Figures 5A and S4A). In contrast to the dynamic awake brain, the quiescent brain manifested as stationary fixed points in PCA space, occupying positions separable from the active brain (Figures 5B and S4B; Movie S2). Notably, this fixed-point attractor was not merely around zero in PCA space but received contributions from the above-described stable GABA neuron activity. Importantly, these features of starvation quiescence fully recapitulated the recently described characteristics of lethargus sleep (Cho and Sternberg, 2014; Nichols et al., 2017), further supporting our conclusion that starvation quiescence is a *C. elegans* sleep state.

Neuronal Population Dynamics Are Robust to Starvation

We next addressed the question how starvation affects brain-wide neuronal activity during awake periods. We hypothesized that neuronal population dynamics should be compromised upon severe starvation, e.g., by reducing signal amplitudes or by reducing the number of neurons recruited to the brain cycle, since both strategies could potentially reduce energy expenditure (Gleichmann and Mattson, 2011). Unexpectedly, a first inspection of our data indicated that the same behavior-related neuronal population dynamics as previously reported for well-fed worms were present irrespective of feeding state (Figures 3B and 3C). We next quantified these observations. A typical feature of neuronal population dynamics are brain-wide correlations, which can be quantified by PCA (Kato et al., 2015). We found that starvation did not alter the principal components (PCs) spectrum obtained from brain activity, showing that most dominant correlations remained intact (Figure 5C). We next set out to quantify global activity levels to test the hypothesis that starvation could alter neuronal signal amplitudes. We calculated the cumulative distributions of mean $\Delta F/F_0$ values for all neurons in each dataset exclusively during active (i.e., non-quiescent) brain episodes, exempting induced activity of O_2-sensory neurons. We found that starvation did not result in a general downregulation of neural activity during active episodes, but instead even subtly upregulated brain activity (Figure 5D). To our surprise, only a few of the identified neurons were regulated by starvation: RMED head motor neurons showed decreased activity, while a set of four anterior ganglion neurons with ambiguous identity (likely URA neurons) showed elevated activity upon starvation (Figures S6A–S6C). Furthermore, in WT fasted animals, neural activity of the sleep-promoting RIS interneuron (Turek et al., 2013, 2016) was bi-modally distributed among awake forward/turn command episodes, i.e., RIS can be found either active or inactive. Starvation shifted this distribution toward increased activity, showing that RIS is found mostly active during awake forward/turn command episodes upon starvation (Figure S6D). We recently reported such a shift in RIS activity levels comparing prelethargus animals with sleep-prone lethargus animals (Nichols et al., 2017). This finding in starved animals supports our previous interpretation that RIS activity levels during wakefulness indicate sleep pressure.

In conclusion, we made the surprising observation that starvation and thus decline in energy supply does not compromise awake brain activity but rather increases the amount of sleep.

DAF-2 Signaling Is Required to Maintain Neuronal Population Dynamics during Fasting

Neuronal population dynamics in fasted *daf-2* animals exhibited the same global features as the ones observed in starved WT animals (Figures 6A, 6B, and S4C). At the single-neuron level, *daf-2*

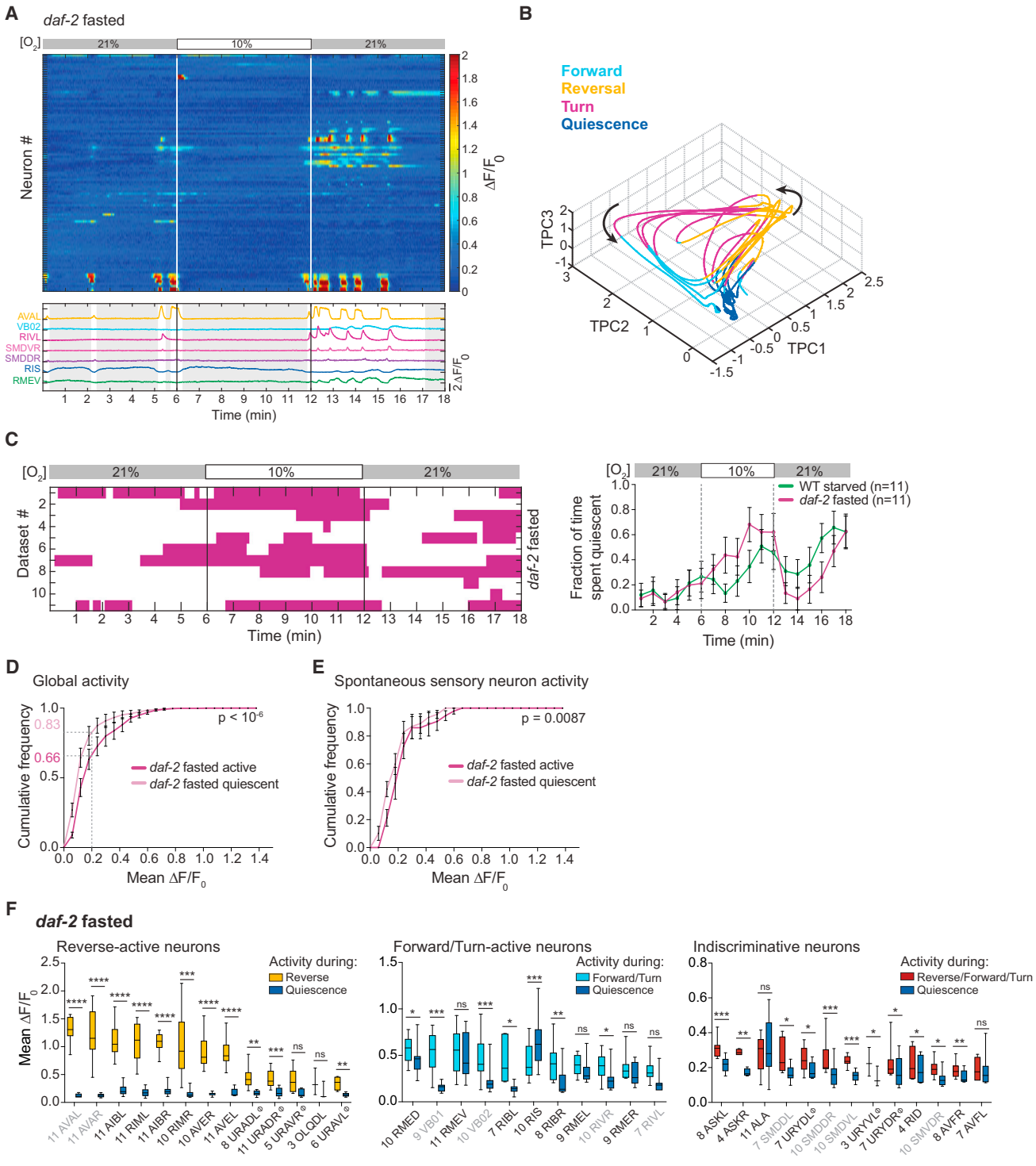

Figure 6. Signaling via DAF-2 Maintains Neural Population Dynamics during Fasting

(A) Top: heat plot of NLS-GCaMP5K fluorescence time series ($\Delta F/F_0$) and example traces (as in Figures 3B and 3C) of a single representative brain-wide imaging recording of a *daf-2* fasted worm. O_2 stimulation as indicated.

(B) Phase plot of first three temporal principal components (TPCs) for the dataset shown in (A). Coloring indicates the respective motor command state, and arrows indicate the direction of time. More examples can be found in Figure S4C.

(C) Left: brain state ethogram of quiescence episodes exhibited by *daf-2* fasted worms in brain-wide imaging recordings. One row corresponds to one recording, each a different animal. Right: traces show mean (±SEM) fraction of time spent quiescent in 1-min bins. n indicates number of recordings. WT starved control (green trace) shows same data as in Figure 3D.

(legend continued on next page)

fasted animals did not show modulation of the neurons tentatively identified as URAs, indicating that the *daf-2* genetic background did not generically recapitulate all effects of starvation on neuronal activity (Figure S6A). Consistent with our behavioral results, the frequency of quiescence episodes in *daf-2* fasted animals corresponded to a profile of WT starved animals. Moreover, unlike WT animals under imaging conditions, suppression of quiescence frequency and upregulation of reversal motor commands by O_2 upshift could be recapitulated in *daf-2* animals (Figures 6C and S5). *Daf-2* mutants are known for their resistance against stressors (e.g., Honda and Honda, 1999; Murakami and Johnson, 1996), suggesting them to be more resilient to the conditions of imaging and immobilization. As described above for WT starved worms, global neural activity as well the contribution from spontaneous sensory neuron activity was downregulated during quiescence in *daf-2* fasted animals; the latter however to a lesser extent (Figures 6D and 6E). The neural sleep signature that was observed in WT starved animals at the level of single neurons was also reiterated in *daf-2* fasted animals (Figure 6F), leading to a fixed point in PCA space (Figure 6B). The distribution of RIS activity levels appeared intermediate between WT fasted and starved animals, suggesting that insulin signaling potentially also affects RIS activity (Figure S6D).

In summary, the maintenance of brain-wide arousal during the initial fasting period requires signaling via the insulin receptor DAF-2.

Starvation and Mutation in *daf-2* Modulate the Activity of Sensory Neurons

Our behavioral genetics results suggested that feeding state and *daf-2* could modulate behavior at the level of sensory neurons. We found that O_2 downshift-evoked responses in BAG neurons (Zimmer et al., 2009) were unaffected by starvation or mutation in *daf-2* (Figures 7A and 7B). In contrast, O_2 upshift-evoked responses in URX neurons (Zimmer et al., 2009), in particular the sustained response component (Busch et al., 2012), were increased by starvation. Mutation in *daf-2* had the opposite effect on URX sensory responses, leading to attenuation (Figures 7C, 7D, and S7).

Recent studies reported *daf-2* requirement for evoked activity in some of the lateral ganglion sensory neurons (Leinwand and Chalasani, 2013; Leinwand et al., 2015). We thus tested whether *daf-2* could affect their spontaneous activity. Based on its stereotypic position, we could unambiguously identify the chemosensory neuron class ASK across multiple datasets. ASK exhibited spontaneous calcium spiking activity (Figure 7E). We found that quiescence suppressed ASK peak amplitudes in both WT starved and *daf-2* fasted animals as compared to active periods (Figure 7F). Furthermore, ASK activity during active periods was lower in *daf-2* fasted than in both WT fasted and starved animals (Figures 7F and S6C).

In summary, ASK and URX neurons provide additional (Leinwand et al., 2015; Leinwand and Chalasani, 2013) examples of neurons that are subject to modulation by *daf-2*, suggesting that regulation of sensory neuron activity is one major mode of DAF-2 action.

DISCUSSION

Insulin Signaling as an Arousal Pathway to Balance Energy Availability and Expenditure

We characterize here an adaptive behavioral strategy that is regulated in dependence of energy availability. Short periods of food deprivation upregulate a behavioral response to the putatively food-indicating cue O_2 (Gray et al., 2004; Hums et al., 2016). Our observations are paralleled by several other studies in *C. elegans* and fruit flies in which acute food deprivation modulates sensory responsiveness, either positively or negatively (Bräcker et al., 2013; Chao et al., 2004; Ezcurra et al., 2011; Ghosh et al., 2016). We hence propose that this transient state of arousal functions to enable active food search when external food sources decline but internal energy supply is still replete. While insulin signaling in *C. elegans* is mostly known for its critical role in regulating life span, metabolism, and reproductive development (for review, see Murphy and Hu, 2013), we show here that it also functions as a regulator of sleep and wakefulness. Neuronal insulin signaling might act as a measure of internal energy resources to maintain the arousal state as long as internal energy supply permits high locomotor activity. In this model, prolonged food deprivation leads to a gradual decline of insulin levels that causes the arousing effect of DAF-2 signaling to diminish and leads to upregulation of *daf-16*-dependent sleep. Importantly, a *daf-16;daf-2* double mutant continues to display reduced sleep levels, suggesting the involvement of other pathways converging onto DAF-16 to be involved in the regulation of sleep upon starvation.

We furthermore describe head-waving as an additional starvation-dependent behavior. While head-waving behavior likely serves other yet-to-be-identified functions, in the present study we show that it often precedes the transition into sleep episodes. In our previous work, we showed that the transition probability to enter lethargus sleep was a function of forward command state duration (Nichols et al., 2017). In analogy, we interpret head-waving as a state of reduced arousal, thereby increasing the probability to transit into starvation sleep. Consistent with this interpretation, the broadly sensory-deficient *osm-9* mutants

(D) Mean (±SEM) cumulative fractional distributions of mean $\Delta F/F_0$ values across all neurons (excluding O_2-responsive neurons) during active or quiescent episodes, in *daf-2* fasted animals. Dashed gray lines denote inactivity cutoff, below which neurons were usually found inactive. Number of recordings (n) = 6.
(E) Mean (±SEM) cumulative fractional distributions of mean $\Delta F/F_0$ values across spontaneously active sensory neurons during active or quiescent episodes. Number of recordings (n) = 6.
(F) Mean $\Delta F/F_0$ of identified neurons during each neuron's principal active state (reverse, forward, or active irrespective of motor state) and the quiescent state in *daf-2* fasted recordings. Boxplots show median, interquartile range, and min to max whiskers. Labels indicate putative neuron IDs. Ambiguous IDs are denoted with Φ (see Experimental Procedures for alternatives). Number of data points for each neuron (n) indicated. Grayed neuronal classes were used for classification of quiescent brain states. Paired t tests (****$p < 0.0001$, ***$p \leq 0.001$, **$p \leq 0.01$, *$p \leq 0.05$; ns, $p > 0.05$).
The p values in (D) and (E) indicate the probability of obtaining an equal or higher difference between the distributions after random shuffling of quiescence episodes; see Experimental Procedures. See also Figures S4–S6.

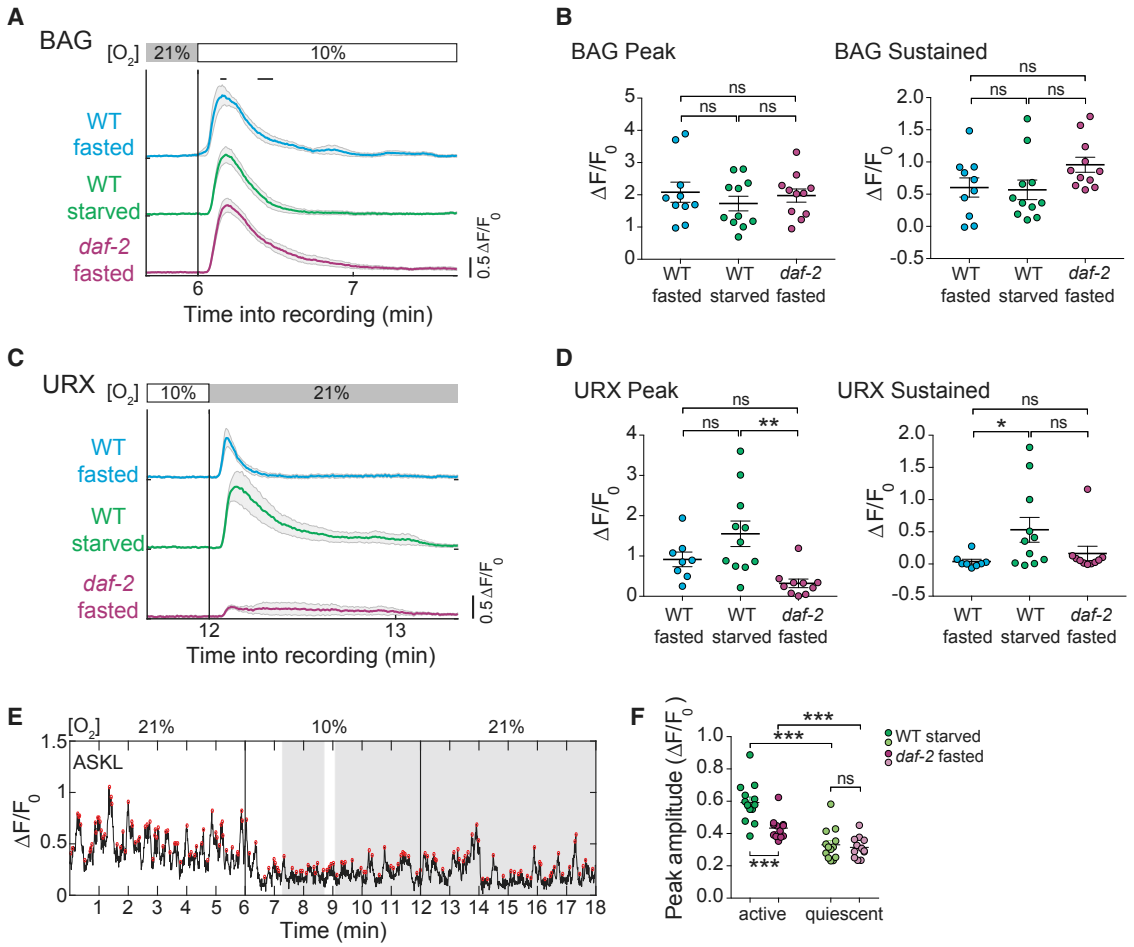

Figure 7. Starvation and Mutation in *daf-2* Modulate the Activity of Sensory Neurons

(A–D) Traces show means (±SEM) $\Delta F/F_0$ of O_2-downshift-sensing BAG neurons (A) and O_2-upshift-sensing URX neurons (C), respectively, extracted from brain-wide imaging recordings. Scatter bar plots (mean ± SEM) of peak (left) and sustained (right) BAG (B) and URX (D) activity. Bars in (A) indicate time periods used for BAG measurements; Figure S7 shows time periods for URX quantification. Number of measured neurons (n): 8-11. Significance of BAG was determined using one-way ANOVA with Sidak's correction (ns, $p > 0.05$), and of URX using Kruskal-Wallis test with Dunn's correction (**$p = 0.0016$, *$p = 0.0297$; ns, $p > 0.05$).

(E) Exemplary Ca^{2+} activity trace of an ASK neuron from the dataset shown in Figure 3C. Gray shadings indicate quiescent brain state episodes. Red circles indicate detected peaks.

(F) Scatter bar plots (mean ± SEM) of mean peak amplitude of ASK activity during active and quiescent periods. Comparisons within one genotype were done using Wilcoxon matched-pairs signed-rank test; comparisons in-between genotypes were made using Mann-Whitney test (***$p \leq 0.001$; ns, $p > 0.9999$). Number of detected ASK neurons for analysis (n): WT starved, n = 13; *daf-2* fasted, n = 12.

See also Figure S7.

failed to enter the head-waving state, leading to largely reduced quiescence levels. These data also suggest that head-waving is triggered by yet-to-be-identified *osm-9*-dependent O_2 sensors and/or other sensory neurons.

In summary, we propose that starvation-induced sleep in worms is a reversible adaptive behavior to conserve energy.

Neuronal Mechanisms Linking Energy State and the Control of Sleep

Recent work described the sleep-promoting RIS interneuron (Turek et al., 2013, 2016) and arousing O_2-sensory circuits as antagonistic regulators of sleep-wake transitions during lethargus (Nichols et al., 2017). In the present study, we show that increased sleep drive upon starvation was likewise associated with elevated RIS activity levels. Remarkably, in fasted *daf-2* animals, which recapitulated many features of starved WT animals, the distribution of RIS activity levels during active brain states was only slightly shifted toward increased activity. This suggests that DAF-2-dependent as well DAF-2-independent mechanisms must contribute to the observed starvation-dependent RIS modulation in WT animals. *Daf-2* and *daf-16* are expressed broadly, with highest expression levels in most of the aforementioned lateral ganglion sensory neurons (Cao et al., 2017). This is consistent with our rescue experiments using the *Posm-9* driver, which is prominently expressed in this sensory neuron cluster (Colbert et al., 1997). In accordance with recent work (Leinwand et al., 2015; Leinwand and Chalasani, 2013), we show that *daf-2* promotes spontaneous and

evoked activity in sensory neurons. This indicates that the absence of *daf-2* signaling increases arousal thresholds sufficiently to promote sleep without elevated RIS activity. However, broad deficiency in sensory neuron signaling like in *osm-9* mutants reduced quiescence, likely because the permissive head-waving state is triggered by still-unknown sensory neurons.

The *C. elegans* genome contains 40 genes for insulin-like ligands (Hobert, 2013; Pierce et al., 2001); therefore, the relevant DAF-2 ligands mediating the arousal state and their tissue expressions remain to be identified. Various individual insulin-like peptides interact in complex signaling networks, resulting in differential effects on biological functions (Fernandes de Abreu et al., 2014). We speculate that starvation results in the downregulation of a specific set of insulin ligands. A loss-of-function mutation in *daf-2* thus presents an extreme manifestation of insulin signaling disruption. Moreover, insulin signaling interacts with other hormonal signaling pathways in worms (Murphy and Hu, 2013). Both could explain why *daf-2* animals do not fully phenocopy starved animals.

Sleep as an Adaptive Strategy to Manage Energy-Expensive Neuronal Signaling

Neural signaling, in particular synaptic transmission, is known to be energy-demanding (Howarth et al., 2012; Rangaraju et al., 2014), yet whether there are specific mechanisms in place that help sustain neuronal signaling in the face of energy scarcity was largely unknown. *C. elegans* neurons lack classic action potentials (Goodman et al., 1998); however, these account for only 15%–22% of the neuronal energy budget in vertebrates. The remainder is allocated to other neuronal signaling mechanisms (Howarth et al., 2012), which are conserved between *C. elegans* and vertebrates (Hobert, 2013), suggesting a similarly high energetic cost of neuronal signaling in worms. We show that neuronal population dynamics, which involve the coordinated activity of a high fraction of all neurons, are largely robust to severe starvation. Our work thus points to a critical importance of these dynamics as they are maintained despite a presumably high energetic cost. Importantly, neuronal population dynamics have been described in several animal species ranging from invertebrates to primates (e.g., Briggman et al., 2005; Bruno et al., 2015; Churchland et al., 2012). We describe that, in worms, the major effect of starvation on brain activity is the frequent and reversible transition into a sleep brain state. Our results suggest that similar adaptation strategies might be applied by larger animals to maintain neuronal network function.

Recent studies reported a cellular mechanism by which *C. elegans* maintains its neural signaling capacity upon energy stress, via synaptic recruitment of metabolic enzymes (Jang et al., 2016). Here, we suggest an additional systemic network-level mechanism. Instead of compromising the dynamic properties of its neuronal networks during active processing, starvation introduces intermittent sleep episodes, during which neuronal activities are systemically downregulated. This downregulation of neuronal signaling in combination with lack of muscle activity thereby potentially allow a reduction in energy consumption.

EXPERIMENTAL PROCEDURES

Further details on all procedures and a comprehensive list of worm strains can be found in Supplemental Experimental Procedures.

Worm Population Behavioral Recordings

The experiments were performed at 20°C, as described previously (Hums et al., 2016; Zimmer et al., 2009). In brief, 1-day-old adult hermaphrodites were transferred to a 56 × 56-mm recording region on bacteria-free nematode growth medium (NGM) agar assay plates. Recordings were acquired at 3 Hz on a 4- to 5-megapixel charge-coupled device (CCD) camera. For starved assays, animals were food-deprived on NGM agar for 16 hr. Temperature-sensitive *daf-2(e1370)* mutants, *daf-2* rescue strains, and corresponding controls were maintained at permissive 16°C and shifted to restrictive 25°C in the evening before the experiment approximately 7 hr before starvation was initiated.

Video Tracking of Animal Behavior and Behavioral State Identification

Tracking and analysis were performed using customized MATLAB scripts that are based on the Parallel Worm Tracker, as described previously (Ramot et al., 2008). We distinguish three behavioral states: an active state, during which the worm is moving; a quiescent state when the worm is completely still; and head-waving, which is characterized by retained dorso-ventral movement of the head/neck region. The states were determined in 1-s bins on the basis of threshold values of speed and instantaneous changes in object eccentricity (see also Figure S1C).

Brain-wide Ca^{2+} Imaging in Microfluidic Device

Animals were immobilized with 1 mM tetramisole in NGM buffer in microfluidic devices that allow controlled O_2 stimuli delivery as previously described (Schrödel et al., 2013). Data were acquired using an inverted spinning disk microscope (UltraViewVoX; PerkinElmer) with an electron-multiplying charge-coupled device (EMCCD) camera (C9100-13; Hamamatsu) at 1.6–2.6 volumes per second.

Statistics

Standard statistical tests were performed in GraphPad Prism 7; all resampling tests were performed using custom scripts in MATLAB. Details on choice and implementation of each statistical test, post-test as well as sample size, displayed data, and p values can be found with each figure legend and Supplemental Experimental Procedures.

SUPPLEMENTAL INFORMATION

Supplemental Information includes Supplemental Experimental Procedures, seven figures, one table, and two movies and can be found with this article online at https://doi.org/10.1016/j.celrep.2017.12.091.

ACKNOWLEDGMENTS

We thank Harris Kaplan and Mara Andrione for critical reading of the manuscript, Richard Latham for generating genetic RMG ablation strains, the National Bioresource Project (NBRP) and *Caenorhabditis* Genetics Center (NIH Office of Research Infrastructure Programs, P40 OD010440) for knockout strains, and the Bargmann, Iino, Zhen, and Mano laboratories for strains and reagents. The research leading to these results has received funding from the European Community's Seventh Framework Programme (FP7/2007-2013)/ERC (grant agreement 281869) and the Research Institute of Molecular Pathology (IMP). M.Z. is supported by the Simons Foundation (grant 324958). The IMP is funded by Boehringer Ingelheim.

AUTHOR CONTRIBUTIONS

S.S. designed and performed experiments, developed analytical methods, and analyzed data. F.M. performed *daf-2* rescue experiments and analyzed

data. M.Z. designed experiments, developed analytical methods, and led the project. S.S. and M.Z. wrote the manuscript.

DECLARATION OF INTERESTS

The authors declare no competing interests.

Received: July 5, 2017
Revised: November 16, 2017
Accepted: December 23, 2017
Published: January 23, 2018

REFERENCES

Alvarenga, T.A.F., Andersen, M.L., Papale, L.A., Antunes, I.B., and Tufik, S. (2005). Influence of long-term food restriction on sleep pattern in male rats. Brain Res. *1057*, 49–56.

Bräcker, L.B., Siju, K.P., Varela, N., Aso, Y., Zhang, M., Hein, I., Vasconcelos, M.L., and Grunwald Kadow, I.C. (2013). Essential role of the mushroom body in context-dependent CO_2 avoidance in *Drosophila*. Curr. Biol. *23*, 1228–1234.

Briggman, K.L., Abarbanel, H.D.I., and Kristan, W.B., Jr. (2005). Optical imaging of neuronal populations during decision-making. Science *307*, 896–901.

Bruno, A.M., Frost, W.N., and Humphries, M.D. (2015). Modular deconstruction reveals the dynamical and physical building blocks of a locomotion motor program. Neuron *86*, 304–318.

Busch, K.E., Laurent, P., Soltesz, Z., Murphy, R.J., Faivre, O., Hedwig, B., Thomas, M., Smith, H.L., and de Bono, M. (2012). Tonic signaling from O_2 sensors sets neural circuit activity and behavioral state. Nat. Neurosci. *15*, 581–591.

Cao, J., Packer, J.S., Ramani, V., Cusanovich, D.A., Huynh, C., Daza, R., Qiu, X., Lee, C., Furlan, S.N., Steemers, F.J., et al. (2017). Comprehensive single-cell transcriptional profiling of a multicellular organism. Science *357*, 661–667.

Chao, M.Y., Komatsu, H., Fukuto, H.S., Dionne, H.M., and Hart, A.C. (2004). Feeding status and serotonin rapidly and reversibly modulate a *Caenorhabditis elegans* chemosensory circuit. Proc. Natl. Acad. Sci. USA *101*, 15512–15517.

Cho, J.Y., and Sternberg, P.W. (2014). Multilevel modulation of a sensory motor circuit during *C. elegans* sleep and arousal. Cell *156*, 249–260.

Choi, S., Taylor, K.P., Chatzigeorgiou, M., Hu, Z., Schafer, W.R., and Kaplan, J.M. (2015). Sensory neurons arouse *C. elegans* locomotion via both glutamate and neuropeptide release. PLoS Genet. *11*, e1005359.

Churchland, M.M., Cunningham, J.P., Kaufman, M.T., Foster, J.D., Nuyujukian, P., Ryu, S.I., and Shenoy, K.V. (2012). Neural population dynamics during reaching. Nature *487*, 51–56.

Colbert, H.A., Smith, T.L., and Bargmann, C.I. (1997). OSM-9, a novel protein with structural similarity to channels, is required for olfaction, mechanosensation, and olfactory adaptation in *Caenorhabditis elegans*. J. Neurosci. *17*, 8259–8269.

Dillon, J., Holden-Dye, L., O'Connor, V., and Hopper, N.A. (2016). Context-dependent regulation of feeding behaviour by the insulin receptor, DAF-2, in *Caenorhabditis elegans*. Invert. Neurosci. *16*, 4.

Dwyer, D.S., and Aamodt, E.J. (2013). Insulin/IGF-1 signaling, including class II/III PI3Ks, β-arrestin and SGK-1, is required in *C. elegans* to maintain pharyngeal muscle performance during starvation. PLoS One *8*, e63851.

Ezcurra, M., Tanizawa, Y., Swoboda, P., and Schafer, W.R. (2011). Food sensitizes *C. elegans* avoidance behaviours through acute dopamine signalling. EMBO J. *30*, 1110–1122.

Fernandes de Abreu, D.A., Caballero, A., Fardel, P., Stroustrup, N., Chen, Z., Lee, K., Keyes, W.D., Nash, Z.M., López-Moyado, I.F., Vaggi, F., et al. (2014). An insulin-to-insulin regulatory network orchestrates phenotypic specificity in development and physiology. PLoS Genet. *10*, e1004225.

Frézal, L., and Félix, M.-A. (2015). *C. elegans* outside the Petri dish. eLife *4*, e05849.

Gallagher, T., Bjorness, T., Greene, R., You, Y.-J., and Avery, L. (2013). The geometry of locomotive behavioral states in *C. elegans*. PLoS One *8*, e59865.

Gems, D., Sutton, A.J., Sundermeyer, M.L., Albert, P.S., King, K.V., Edgley, M.L., Larsen, P.L., and Riddle, D.L. (1998). Two pleiotropic classes of daf-2 mutation affect larval arrest, adult behavior, reproduction and longevity in *Caenorhabditis elegans*. Genetics *150*, 129–155.

Gendrel, M., Atlas, E.G., and Hobert, O. (2016). A cellular and regulatory map of the GABAergic nervous system of *C. elegans*. eLife *5*, e17686.

Ghosh, R., and Emmons, S.W. (2008). Episodic swimming behavior in the nematode *C. elegans*. J. Exp. Biol. *211*, 3703–3711.

Ghosh, D.D., Sanders, T., Hong, S., McCurdy, L.Y., Chase, D.L., Cohen, N., Koelle, M.R., and Nitabach, M.N. (2016). Neural architecture of hunger-dependent multisensory decision making in *C. elegans*. Neuron *92*, 1049–1062.

Gleichmann, M., and Mattson, M.P. (2011). Neuronal calcium homeostasis and dysregulation. Antioxid. Redox Signal. *14*, 1261–1273.

Goodman, M.B., Hall, D.H., Avery, L., and Lockery, S.R. (1998). Active currents regulate sensitivity and dynamic range in *C. elegans* neurons. Neuron *20*, 763–772.

Gray, J.M., Karow, D.S., Lu, H., Chang, A.J., Chang, J.S., Ellis, R.E., Marletta, M.A., and Bargmann, C.I. (2004). Oxygen sensation and social feeding mediated by a *C. elegans* guanylate cyclase homologue. Nature *430*, 317–322.

Hill, A.J., Mansfield, R., Lopez, J.M.N.G., Raizen, D.M., and Van Buskirk, C. (2014). Cellular stress induces a protective sleep-like state in *C. elegans*. Curr. Biol. *24*, 2399–2405.

Hobert, O. (2013). The neuronal genome of *Caenorhabditis elegans*. WormBook *2013*, 1–106.

Honda, Y., and Honda, S. (1999). The *daf-2* gene network for longevity regulates oxidative stress resistance and Mn-superoxide dismutase gene expression in *Caenorhabditis elegans*. FASEB J. *13*, 1385–1393.

Howarth, C., Gleeson, P., and Attwell, D. (2012). Updated energy budgets for neural computation in the neocortex and cerebellum. J. Cereb. Blood Flow Metab. *32*, 1222–1232.

Hums, I., Riedl, J., Mende, F., Kato, S., Kaplan, H.S., Latham, R., Sonntag, M., Traunmüller, L., and Zimmer, M. (2016). Regulation of two motor patterns enables the gradual adjustment of locomotion strategy in *Caenorhabditis elegans*. eLife *5*, e14116.

Iwanir, S., Tramm, N., Nagy, S., Wright, C., Ish, D., and Biron, D. (2013). The microarchitecture of *C. elegans* behavior during lethargus: homeostatic bout dynamics, a typical body posture, and regulation by a central neuron. Sleep (Basel) *36*, 385–395.

Jang, S., Nelson, J.C., Bend, E.G., Rodríguez-Laureano, L., Tueros, F.G., Cartagenova, L., Underwood, K., Jorgensen, E.M., and Colón-Ramos, D.A. (2016). Glycolytic enzymes localize to synapses under energy stress to support synaptic function. Neuron *90*, 278–291.

Kato, S., Kaplan, H.S., Schrödel, T., Skora, S., Lindsay, T.H., Yemini, E., Lockery, S., and Zimmer, M. (2015). Global brain dynamics embed the motor command sequence of *Caenorhabditis elegans*. Cell *163*, 656–669.

Keene, A.C., Duboué, E.R., McDonald, D.M., Dus, M., Suh, G.S.B., Waddell, S., and Blau, J. (2010). Clock and cycle limit starvation-induced sleep loss in *Drosophila*. Curr. Biol. *20*, 1209–1215.

Kimura, K.D., Tissenbaum, H.A., Liu, Y., and Ruvkun, G. (1997). daf-2, an insulin receptor-like gene that regulates longevity and diapause in *Caenorhabditis elegans*. Science *277*, 942–946.

Landauer, R. (1961). Irreversibility and heat generation in the computing process. IBM J. Res. Dev. *5*, 183–191.

Laughlin, S.B. (2001). Energy as a constraint on the coding and processing of sensory information. Curr. Opin. Neurobiol. *11*, 475–480.

Leinwand, S.G., and Chalasani, S.H. (2013). Neuropeptide signaling remodels chemosensory circuit composition in *Caenorhabditis elegans*. Nat. Neurosci. *16*, 1461–1467.

Leinwand, S.G., Yang, C.J., Bazopoulou, D., Chronis, N., Srinivasan, J., and Chalasani, S.H. (2015). Circuit mechanisms encoding odors and driving aging-associated behavioral declines in *Caenorhabditis elegans*. eLife *4*, e10181.

Longden, K.D., Muzzu, T., Cook, D.J., Schultz, S.R., and Krapp, H.G. (2014). Nutritional state modulates the neural processing of visual motion. Curr. Biol. *24*, 890–895.

Macosko, E.Z., Pokala, N., Feinberg, E.H., Chalasani, S.H., Butcher, R.A., Clardy, J., and Bargmann, C.I. (2009). A hub-and-spoke circuit drives pheromone attraction and social behaviour in *C. elegans*. Nature *458*, 1171–1175.

McCloskey, R.J., Fouad, A.D., Churgin, M.A., and Fang-Yen, C. (2017). Food responsiveness regulates episodic behavioral states in *Caenorhabditis elegans*. J. Neurophysiol. *117*, 1911–1934.

Mink, J.W., Blumenschine, R.J., and Adams, D.B. (1981). Ratio of central nervous system to body metabolism in vertebrates: its constancy and functional basis. Am. J. Physiol. *241*, R203–R212.

Murakami, S., and Johnson, T.E. (1996). A genetic pathway conferring life extension and resistance to UV stress in *Caenorhabditis elegans*. Genetics *143*, 1207–1218.

Murphy, C.T., and Hu, P.J. (2013). Insulin/insulin-like growth factor signaling in *C. elegans*. WormBook *2013*, 1–43.

Nichols, A.L.A., Eichler, T., Latham, R., and Zimmer, M. (2017). A global brain state underlies *C. elegans* sleep behavior. Science *356*, eaam6851.

Persson, A., Gross, E., Laurent, P., Busch, K.E., Bretes, H., and de Bono, M. (2009). Natural variation in a neural globin tunes oxygen sensing in wild *Caenorhabditis elegans*. Nature *458*, 1030–1033.

Pierce, S.B., Costa, M., Wisotzkey, R., Devadhar, S., Homburger, S.A., Buchman, A.R., Ferguson, K.C., Heller, J., Platt, D.M., Pasquinelli, A.A., et al. (2001). Regulation of DAF-2 receptor signaling by human insulin and ins-1, a member of the unusually large and diverse *C. elegans* insulin gene family. Genes Dev. *15*, 672–686.

Plaçais, P.-Y., and Preat, T. (2013). To favor survival under food shortage, the brain disables costly memory. Science *339*, 440–442.

Raizen, D.M., Lee, R.Y.N., and Avery, L. (1995). Interacting genes required for pharyngeal excitation by motor neuron MC in *Caenorhabditis elegans*. Genetics *141*, 1365–1382.

Raizen, D.M., Zimmerman, J.E., Maycock, M.H., Ta, U.D., You, Y.-J., Sundaram, M.V., and Pack, A.I. (2008). Lethargus is a *Caenorhabditis elegans* sleep-like state. Nature *451*, 569–572.

Ramot, D., Johnson, B.E., Berry, T.L., Jr., Carnell, L., and Goodman, M.B. (2008). The Parallel Worm Tracker: a platform for measuring average speed and drug-induced paralysis in nematodes. PLoS ONE *3*, e2208.

Rangaraju, V., Calloway, N., and Ryan, T.A. (2014). Activity-driven local ATP synthesis is required for synaptic function. Cell *156*, 825–835.

Schrödel, T., Prevedel, R., Aumayr, K., Zimmer, M., and Vaziri, A. (2013). Brain-wide 3D imaging of neuronal activity in *Caenorhabditis elegans* with sculpted light. Nat. Methods *10*, 1013–1020.

Sexstone, A.J., Revsbach, N.P., Parkin, T.B., and Tiedje, J.M. (1985). Direct measurement of oxygen profiles and denitrification rates in soil aggregates. Soil Sci. Soc. Am. J. *49*, 645–651.

Slocumb, M.E., Regalado, J.M., Yoshizawa, M., Neely, G.G., Masek, P., Gibbs, A.G., and Keene, A.C. (2015). Enhanced sleep is an evolutionarily adaptive response to starvation stress in *Drosophila*. PLoS One *10*, e0131275.

Sze, J.Y., Victor, M., Loer, C., Shi, Y., and Ruvkun, G. (2000). Food and metabolic signalling defects in a *Caenorhabditis elegans* serotonin-synthesis mutant. Nature *403*, 560–564.

Turek, M., Lewandrowski, I., and Bringmann, H. (2013). An AP2 transcription factor is required for a sleep-active neuron to induce sleep-like quiescence in *C. elegans*. Curr. Biol. *23*, 2215–2223.

Turek, M., Besseling, J., Spies, J.-P., König, S., and Bringmann, H. (2016). Sleep-active neuron specification and sleep induction require FLP-11 neuropeptides to systemically induce sleep. eLife *5*, e12499.

Waterson, M.J., and Horvath, T.L. (2015). Neuronal regulation of energy homeostasis: beyond the hypothalamus and feeding. Cell Metab. *22*, 962–970.

White, J.G., Southgate, E., Thomson, J.N., and Brenner, S. (1986). The structure of the nervous system of the nematode *Caenorhabditis elegans*. Philos. Trans. R. Soc. Lond. B Biol. Sci. *314*, 1–340.

Witham, E., Comunian, C., Ratanpal, H., Skora, S., Zimmer, M., and Srinivasan, S. (2016). *C. elegans* body cavity neurons are homeostatic sensors that integrate fluctuations in oxygen availability and internal nutrient reserves. Cell Rep. *14*, 1641–1654.

Zimmer, M., Gray, J.M., Pokala, N., Chang, A.J., Karow, D.S., Marletta, M.A., Hudson, M.L., Morton, D.B., Chronis, N., and Bargmann, C.I. (2009). Neurons detect increases and decreases in oxygen levels using distinct guanylate cyclases. Neuron *61*, 865–879.